

## Supporting Information for

Quantitative mechanical stimulation of GPR68 using a novel 96 well flow plugin

Philipp Segeritz<sup>1,2</sup>, Kirill Kolesnik<sup>1</sup>, Daniel J. Scott<sup>2,3\*</sup>, David J. Collins<sup>1,4\*</sup>

<sup>1</sup>Department of Biomedical Engineering, The University of Melbourne, Parkville, VIC 3010, Victoria, Australia

<sup>2</sup>The Florey Institute of Neuroscience and Mental Health, The University of Melbourne, 30 Royal Parade, Parkville, VIC 3052, Australia.

<sup>3</sup>Department of Biochemistry and Pharmacology, The University of Melbourne, Parkville, VIC 3010, Australia

<sup>4</sup>The Graeme Clark Institute, The University of Melbourne, Parkville, VIC, 3010, Australia

\*Corresponding Authors: Daniel J. Scott, David J. Collins

Email: [daniel.scott@florey.edu.au](mailto:daniel.scott@florey.edu.au), [david.collins@unimelb.edu.au](mailto:david.collins@unimelb.edu.au)

### This PDF file includes:

Supporting Notes 1 to 3 Figures S1 to S2

## Supplementary Information Note 1:

### Numerical analysis governing equations

Computational fluid dynamics (CFD) analysis was used to model fluid flow in the domain shown in Fig. S1a. At the volumetric flow rate of  $Q = 8.3 \cdot 10^{-3} \text{ m}^3/\text{s}$  the Reynolds number was estimated to reach 1.4 at the inlet cross section. Due to the diverging shape of the computational domain downstream, the Reynolds number was predicted to be under 1.4 in the entire domain, what allows to assure laminar flow regime throughout. Stationary, linearized governing equations of continuity and momentum conservation (Navier-Stokes) for incompressible flow are considered, with

$$\rho \nabla \cdot \mathbf{u} = 0, \quad (\text{S1,1})$$

$$\rho(\mathbf{u} \cdot \nabla)\mathbf{u} = \nabla \cdot (-p\mathbf{I} + \mu(\nabla\mathbf{u} + (\nabla\mathbf{u})^T)), \quad (\text{S1,2})$$

where  $\rho = 997 \text{ kg/m}^3$  is the mass density,  $\mathbf{u}$  fluid velocity, and  $p$  is pressure,  $\mathbf{I}$  unity matrix,  $\mu = 0.75 \text{ mPa s}$  dynamic viscosity.

The governing equations were complemented with flow rate boundary condition at the inlet  $\partial\Omega$ :

$$-\int_{\partial\Omega} \mathbf{u} \cdot \mathbf{n} dS = Q, \quad (\text{S1,3})$$

where  $\mathbf{n}$  is the unit normal with respect to the boundary,  $Q$  is the total volumetric flow rate. A pressure boundary condition is applied at the outlet:

$$(-p\mathbf{I} + \mu(\nabla\mathbf{u} + (\nabla\mathbf{u})^T))\mathbf{n} = 0. \quad (\text{S1,4})$$

To realize the radial symmetry of the domain, a slip boundary condition was applied on the side walls, where

$$\mathbf{u} \cdot \mathbf{n} = 0. \quad (\text{S1,5})$$

A non-slip boundary conditions are applied at fluid-solid interfaces:

$$\mathbf{u} = 0. \quad (\text{S1,6})$$

This system was solved using COMSOL Multiphysics 5.5 (COMSOL, Stockholm, Sweden). Velocity and pressure fields were discretized with a piecewise linear interpolation. Generalized

minimum residual (GMRES) iterative stationary solver based on the Krylov subspace method was used for the system analysis.

### Computational mesh analysis

Tetrahedral mesh elements were used for the domain discretization (Fig. S2b). A mesh convergence study was conducted using the approach from Devendran et al.<sup>4</sup> and Muller et al..<sup>5</sup> A convergence function  $C(g)$  can be written as follows:

$$C(g) = \sqrt{\frac{\int (u_g - u_{ref})^2 dx dy dz}{\int (u_{ref})^2 dx dy dz}}, \quad (S1,7)$$

where  $g$  is the current solution, ref is a reference solution. Current and reference solutions have maximum mesh element size of  $d_m$  and  $d_{m,ref} = 0.03$  mm respectively with additional mesh refinement in the fluid boundary layer. Fig. S\_c shows the convergence function decay with mesh refinement. Convergence threshold of  $C < 0.005$  realized in a computational meshes with  $d_m = 0.07$  mm used in this study (Fig. S1b).

## Supplementary Information Note 2:

### Analytical calculation of the flow velocities and shear rates

To assess the strength of the mechanical stimulus cells would experience in this device, flow rates and shear rates have been estimated following Rong Tsu Yen's analytical study on radial flow between two parallel discs<sup>32</sup>. Figure 1E shows the flow at the bottom of the well and significant dimension such as the inlet radius  $r_1$ , the plugin radius  $r_2$  and the channel height  $2*b$ . It was assumed that the fluid is Newtonian and incompressible and that the flow is steady and laminar. Furthermore, the following variables were defined as:

$r$	=	radial distance at any given point	(in mm)
$z$	=	height in the channel at any point	(in mm)
$b$	=	channel height/2	(in mm)
$r_1$	=	inlet radius	(in mm)
$r_2$	=	plugin radius at its lowest point	(in mm)
$v_r$	=	radial velocity component	(in mm)
$v_\theta$	=	peripheral velocity component	(in mm)
$v_z$	=	z-directional velocity component	(in mm)
$P$	=	pressure	(in $N/m^2$ )
$\Delta P$	=	pressure difference	(in $N/m^2$ )
$\mu$	=	dynamic viscosity	(in $\frac{N}{m^2} s$ )
$Q$	=	volumetric flow	(in $m^3/s$ )
$\dot{\gamma}$	=	shear rate	(in $1/s$ )
$\tau$	=	shear stress	(in $N/m^2$ )

Under the assumption of radial flow  $V_\theta = V_z = 0$ , one can follow Yen [1] and use the Navier Stokes equation to devise the following differential equation describing the flow velocity for  $r_1 < r < r_2$  and  $-b < z < b$ .

Equation 1, Flow velocity:

$$V_r(r, z) = \frac{b^2 \Delta P}{2\mu r \ln(r_2/r_1)} \left[ 1 - \left( \frac{z}{b} \right)^2 \right] \quad (\text{S2,1})$$

The pressure difference ( $\Delta P$ ) is unknown. But it is a function of the volumetric flow rate. Since the volumetric flow rate is determined by the syringe pump, it is a known variable and can be used to eliminate the pressure difference from the equation. The volumetric flow rate can be expressed by integrating the velocity profile from  $-b$  to  $+b$  over the circumference.

$$Q = \int_{-b}^b v_r * 2\pi r \, dz \quad (\text{S2,2})$$

Substituting the velocity profile from equation 1 gives:

Equation 2, Volumetric flow rate:

$$\begin{aligned} Q &= \int_{-b}^b 2\pi r \frac{b^2 \Delta P}{2\mu r \ln(r_2/r_1)} \left[ 1 - \left( \frac{z}{b} \right)^2 \right] dz \\ &= \frac{\pi b^2 \Delta P}{\mu \ln(r_2/r_1)} \left[ z - \frac{z^3}{3b^2} \right]_{-b}^b \\ &= \frac{4\pi b^3 \Delta P}{3\mu \ln(r_2/r_1)} \quad (\text{S2,3}) \end{aligned}$$

Solving equation 2 for  $\Delta P$  gives:

$$\Delta P = \frac{3Q\mu \ln(r_2/r_1)}{4\pi b^3} \quad (\text{S2,4})$$

Substituting  $\Delta P$  in equation 1 enables the calculation of the flow velocity:

$$V_r(r, z) = \frac{b^2 \frac{3Q\mu \ln(r_2/r_1)}{4\pi b^3}}{2\mu r \ln(r_2/r_1)} \left[ 1 - \left(\frac{z}{b}\right)^2 \right]$$

$$= \frac{3Q}{8\pi b r} \left[ 1 - \left(\frac{z}{b}\right)^2 \right] \quad (\text{S2,5})$$

To obtain the shear rate, the flow velocity ( $V_r$ ) was differentiated:

$$\dot{\gamma} = \frac{dV_r}{d(z)} = -2z \frac{3Q}{8\pi b^3 r}$$

(S2,6)

Multiplying the shear rate with the fluids dynamic viscosity  $\mu$  gives the following shear stress equation.

Equation 1, Shear stress:

$$\tau = -2z \mu \frac{3Q}{8\pi b^3 r} \quad (\text{S2,7})$$

To obtain the shear stress at the bottom of the well we can insert the following parameters into this equation.

$$z = -b$$

$$b = 100 \mu\text{m} \quad (\text{distance to bottom of the well})$$

$$\mu = 0.75 \text{ mPa s} \quad (\text{dynamic viscosity of extracellular solution})$$

$$\tau = -2 * (-b)\mu \frac{3Q}{8\pi b^2 r} = \mu \frac{6Q}{8\pi b^2 r} \quad (\text{S2,8})$$

This enables the calculation of shear stress at different points on the bottom of the well for a known injected volumetric flow rate (e.g., 50  $\mu\text{l}/\text{min}$ ).

$$Q = 50 \mu\text{l}/\text{min} = 8.3 * 10^{-10} \text{ m}^3/\text{s}$$

$$\tau = \frac{9Ns * Q}{16\pi m^4 r} * 10^6 = \frac{9Ns * 8.3 \text{ m}^3/\text{s}}{16\pi m^4 r} * 10^{-4} = \frac{9N * 8.3}{16m\pi r} * 10^{-4}$$

### **Supplementary Information Note 3:**

#### **Supplementary Video 1**

This video presents the flow-induced R-GECO1 fluorescence response in HEK293 cells expressing the mechanosensitive protein GPR68. Utilizing the flow plugin, the images were recorded from the bottom of the well with an Inverted Fluorescence Microscope IX73 (Olympus, Japan). The exposure time was selected to be 1 second. This video is played back at 10 frames per second, effectively increasing the playback speed by a factor of 10. A channel height of 200  $\mu\text{m}$  was chosen, and this was paired with a flow injection rate of 50  $\mu\text{l}/\text{min}$ , sustained for a 20-second interval. The injection was initiated 10 seconds after the commencement of the recording. The white scale bar in the video corresponds to a distance of 200  $\mu\text{m}$ . The injection inlet is situated in the lower left corner of the field of view, with its outer boarder discernible as an arc. The high magnification employed results in the circular flow off area and the feet being outside the boundaries of the observed area. Elevated R-GECO1 fluorescence is evident in many cells following the initial application of flow. Subsequent gradual declines return the fluorescence to baseline levels during the course of the recording. This observed effect seems to diminish with increasing distance to the inlet located at the bottom left of the field of view, with the area directly beneath the inlet forming a noticeable exception.

## Supplementary Figures

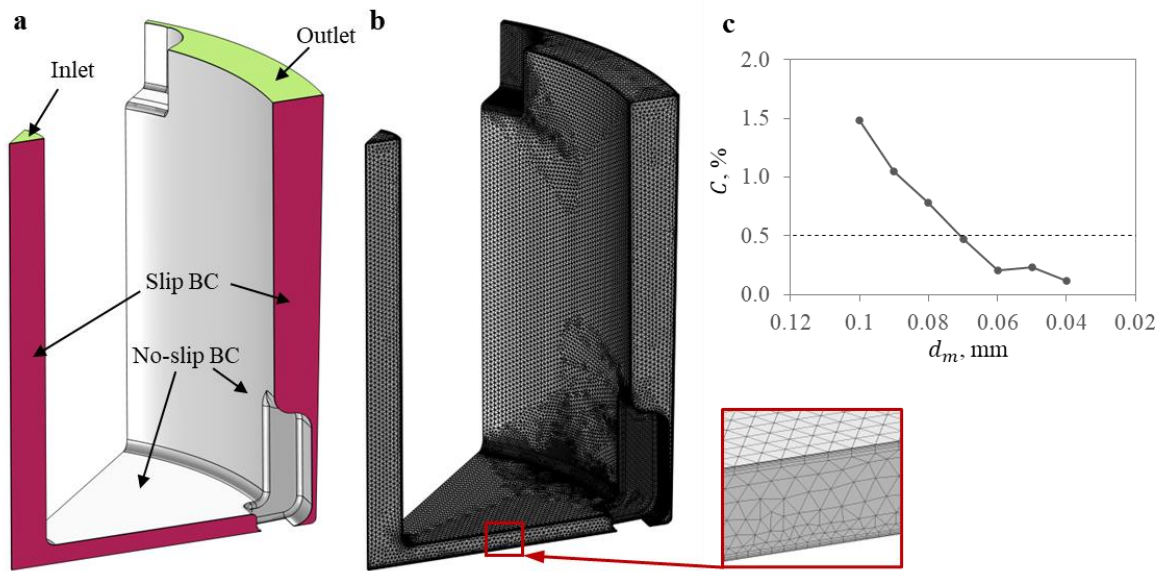


**Fig. S1:** Computational domain (a). Computational mesh (b). Mesh convergence analysis (c).

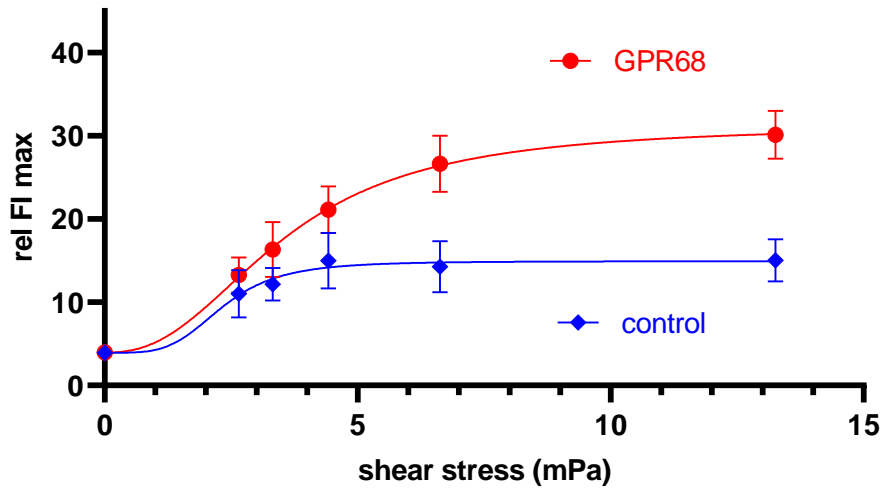


**Fig. S2:** Maximal relative fluorescence intensity for  $50 < t < 100$  interval plotted against orbital diameter dependent shear stress.

### References

- [1] Yen, R. T. Radial flow between two parallel discs. (Kansas State University, 1965).